

Computational Feasibility Analysis of Electrochemotherapy With Novel Needle-Electrode Arrays for the Treatment of Invasive Breast Ductal Carcinoma

Technology in Cancer Research & Treatment
Volume 17: 1-13
© The Author(s) 2018
Article reuse guidelines:
sagepub.com/journals-permissions
DOI: 10.1177/1533033818794939
journals.sagepub.com/home/tct
 SAGE

Adriana Leticia Vera-Tizatl, MSAT¹, Claudia Elizabeth Vera-Tizatl, MSc²,
Arturo Vera-Hernández, PhD¹, Lorenzo Leija-Salas, PhD¹,
Sergio Rodríguez, MD³, Damijan Miklavčič, PhD⁴, and Bor Kos, PhD⁴

Abstract

Breast cancer represents a rising problem concerning public health worldwide. Current efforts are aimed to the development of new minimally invasive and conservative treatment procedures for this disease. A treatment approach for invasive breast ductal carcinoma could be based on electroporation. Hence, in order to determine the effectiveness of electrochemotherapy in the treatment of this disease, 12 electrode models were investigated on realistic patient-specific computational breast models of 3 patients diagnosed by Digital Breast Tomosynthesis imaging. The electrode models exhibit 4, 5, and 6 needles arranged in 4 geometric configurations (delta, diamond, and star) and 3 different needle spacing resulting in a total of 12 needle-electrode arrays. Electric field distribution in the tumors and a surrounding safety margin of 1 cm around the tumor edge is computed using the finite element method. Efficiency of the electrode arrays was determined hierarchically based on (1) percentage of tumor volume reversibly electroporated, (2) percentage of tumor volume irreversibly electroporated, (3) percentage of treated safety margin volume, (4) minimal invasiveness, that is, minimal number of electrodes used, (5) minimal activated electrode pairs, and (6) minimal electric current. Results show that 3 electrode arrays (4 needle-delta, 5 needle-diamond, and 6 needle-star) with fixed-geometry configuration could be used in the treatment with electrochemotherapy of invasive breast ductal carcinomas ranging from 1 to 5 cm³ along with a surrounding safety margin of 1 cm.

Keywords

breast cancer, computational breast model, electroporation, finite element modeling, safety margin

Abbreviations

BI-RADS, breast imaging reporting and data system; CC, cranial caudal; C-P, central to peripheral; D, diagonal electrodes; DBT, digital breast tomosynthesis; E, electrode; ECT, electrochemotherapy; ER, estrogen receptors; HER-2, hormone epidermal growth factor receptor 2; IDC, invasive ductal carcinoma; IRE, irreversible electroporation; MLO, medio-lateral oblique; P-P, peripheral to peripheral; PR, progesterone receptors; SM, safety margin; 2-D, 2-dimensional; 3-D, 3-dimensional; 4DeI, 4 needle-delta configuration-set 1; 4DiI, 4 needle-diamond configuration-set 1; 5DiI, 5 needle-diamond configuration-set 1;

¹ Department of Electrical Engineering, Centro de Investigación y de Estudios Avanzados del Instituto Politécnico Nacional (CINVESTAV-IPN), Mexico City, Mexico

² Department of Infectomics and Molecular Pathogenesis, Centro de Investigación y de Estudios Avanzados del Instituto Politécnico Nacional (CINVESTAV-IPN), Mexico City, Mexico

³ Institute of Breast Diseases, FUCAM, Mexico City, Mexico

⁴ Faculty of Electrical Engineering, University of Ljubljana, Ljubljana, Slovenia

Corresponding Author:

Bor Kos, University of Ljubljana, Trzaska 25, Ljubljana, N/A 1000, Ljubljana, Slovenia.

Email: bor.kos@fe.uni-lj.si



Creative Commons Non Commercial CC BY-NC: This article is distributed under the terms of the Creative Commons Attribution-NonCommercial 4.0 License (<http://www.creativecommons.org/licenses/by-nc/4.0/>) which permits non-commercial use, reproduction and distribution of the work without further permission provided the original work is attributed as specified on the SAGE and Open Access pages (<https://us.sagepub.com/en-us/nam/open-access-at-sage>).

6St1, 6 needle-star configuration-set 1; 4De2, 4 needle-delta configuration-set 2; 4Di2, 4 needle-diamond configuration-set 2; 5Di2, 5 needle-diamond configuration-set 2; 6St2, 6 needle-star configuration-set 2; 4De3, 4 needle-delta configuration-set 3; 4Di3, 4 needle-diamond configuration-set 3; 6St3, 6 needle-star configuration-set 3

Received: December 27, 2017; Revised: June 24, 2018; Accepted: July 24, 2018.

Introduction

Breast cancer, due to malignant tumors in women older than 25, represents the first cause of death of women in Mexico since 2006. Its recurrence has increased 49.5% during the last 2 decades; about 45% of total cases are diagnosed in stages III and IV, and 11% are women younger than 40 years. Remarkably, the survival rate for the latter group is lower compared to the older population.¹

The most common histologic subtypes of breast tumors are ductal carcinoma, in situ and invasive (IDC), and lobular carcinoma, in situ and invasive. Both of them account for the 90% (80% and 10%, respectively) of all breast tumors.^{1,2} Breast cancer is a major problem concerning public health worldwide, and current efforts are aimed at controlling known risk factors, establishment of early detection programs, and the development of new minimally invasive and conservative treatment procedures for this disease.^{1,3}

The techniques currently used for treating breast cancer are neoadjuvant chemotherapy, radiotherapy, hormonal therapy, and surgical procedures, which include lumpectomy and mastectomy. Interestingly, 10% to 20% of diagnosed breast cancers are considered as triple negative breast cancer. For this type of tumors, treatments like hormone therapy and drugs that target estrogen, progesterone, and HER-2 receptors are ineffective, leaving chemotherapy as the only treatment. This characteristic makes these tumors more aggressive and difficult to treat.

Electroporation, or electroporabilization, may be a novel approach for treating invasive ductal carcinoma because electroporation of the plasma membrane of living cells increases the uptake of nonpermeant or poorly permeant molecules once the cells had been exposed to short and strong electric pulses. Moreover, it is possible to permeabilize the cell plasma membranes while preserving their viability, which allows them to return to their natural state in a process called reversible electroporation.⁴ However, if the electric field is stronger than the irreversible threshold, it leads to cell death caused by irreversible electroporation (IRE).⁵ Reversible electroporation has been used for many clinical applications, such as the introduction of drugs into cells, electrochemotherapy, gene delivery to tissue, and transdermal delivery of drugs and genes.⁶⁻¹¹ Electrochemotherapy (ECT) enables the potentiation of effectiveness of chemotherapeutic drugs bleomycin by a factor of up to 1000 and cisplatin by a factor of up to 80.^{6-9,12} Electrochemotherapy is a local minimally invasive treatment that has been proven to be effective in cutaneous and subcutaneous tumors with different histologies.¹³⁻¹⁶ Most frequently, ECT represents

a palliative treatment in patients with cancer having progressive disease (stage IV); the therapeutic goal is improving the quality of life (bleeding and pain relief) during terminal phase due to the lack of suitable treatment to prolong overall survival.^{17,18} Electrochemotherapy has been proven to be highly effective in palliative treatment of cutaneous tumors including cutaneous tumors from breast cancer and chest wall recurrences of breast cancer.¹⁷⁻¹⁹ Because of its benefits, such as high specificity for targeting cancer cells and capacity for preserving the innate immune response, its use is therefore being extended to the treatment of internal tumors.²⁰⁻²⁴ Clinical experiences regarding the treatment of liver and bone metastases, soft tissue sarcomas, brain tumors, and colorectal and esophageal tumors have been reported.²⁰ Electrochemotherapy of breast cancer metastases to the skin and subcutaneous tissues has also been reported showing encouraging outcomes.^{17,25-28} However, to our best knowledge, there are only 2 works that address the treatment of primary breast cancer with ECT, that is, (1) an infiltrative lobular carcinoma in a single elderly patient, inoperable for neoplastic infiltration of the chest wall and undergoing preoperative (attempt of cytoreduction) and intraoperative ECT prior to radical mastectomy²⁹ and (2) a single clinical case of unifocal ductal breast cancer that reports reduced efficacy of the ECT treatment with 5 needle electrodes.³⁰ Both studies performed ECT through Cliniporator (IGEA SpA, Carpi, Italy) and operating standard procedures for Electrochemotherapy.^{17,18} These results lead us to suggest that ECT may displace neoadjuvant chemotherapy and/or surgery in the treatment of breast cancer and have encouraged the development of better electrode configurations along with an adequate pretreatment planning based on numerical models for the treatment of invasive breast ductal carcinoma with ECT.³⁰

Treatment of breast cancer has also been addressed by IRE. Investigation on this issue has been carried out on one hand in vitro in order to establish a baseline estimate of electric field necessary for IRE treatment of breast carcinomas.³¹ On the other hand, in vivo studies have been reported in animal models comprising nude mice³² and rabbits.³³ The results reported in these works suggest that IRE may be a promising approach for patients with breast cancer who are not eligible for surgical excision. In addition, numerical modeling of electric field distribution represents a useful tool to validate the required voltage to fully expose the target to the electric field determined from in vitro experiments. Nonetheless, more experimental evidence regarding the treatment of breast cancer with IRE is required, since reports on this field remain limited.³¹⁻³⁴

This work researched the feasibility of using electrochemotherapy for the treatment of IDC in realistic breast models based on digital breast tomosynthesis (DBT) images with a universal electrode array to assure the electroporation of the entire target volume.³⁵ In addition to the tumor treatment, eradication of some surrounding tumor tissue is desirable, since tumor cells that have an infiltrative-like histological type spread diffusely throughout the healthy tissue. In order to achieve the destruction of the tumor and the eradication of some surrounding healthy tissue efficiently, 12 electrode arrays in 4 configurations were used for modeling electroporation of tumors corresponding to 3 representative clinical cases. Novel electrode arrays, which included a central intratumoral needle, are proposed in this work, and the results are compared to those obtained with electrode arrays without intratumoral needles in order to establish a suitable protocol for electrochemotherapy of invasive breast ductal carcinomas and a safety margin of healthy tissue.

Methods

Breast Computational Model

Imaging studies were approved by the Scientific-Ethics Committee of the Institute of Breast Diseases-FUCAM (approval number 2017/14). All patients provided verbal consent to be subjected to the imaging studies. Three representative clinical cases of women diagnosed with invasive breast ductal carcinoma without previous treatment, hence corresponding to primary deep-seated tumors, were analyzed to evaluate their treatment with electrochemotherapy. In all cases, diagnosis was done by DBT, Giotto Tomo, IMS (slice thickness 1 mm and pixel size 0.1 mm).

Mammography has been used as the primary detection tool for breast abnormalities, but nowadays it is being replaced by DBT. Digital Breast Tomosynthesis is a 3-dimensional (3-D) imaging technology that involves acquisition of images of a stationary compressed breast at multiple X-ray source angles during a short scan. Typically, the X-ray tube is rotated 10° to 20°, and 10° to 20° exposures are made approximately at every 1° of rotation during a total scan of 5 seconds or less. Individual images are then reconstructed into a series of thin, high-resolution slices with a separation of 1 mm. Tissues that overlap in 2-D conventional mammography and hide pathologies are less likely to be obscured using tomosynthesis. The cross-sectional 3-D slice allows a clearer visualization of the lesion.³⁶ Digital breast tomosynthesis differs from other 3-D imaging modalities in that orthogonal multiplanar reconstructions such as sagittal, axial, and coronal views from the transverse tomosynthesis image sets cannot be generated. Instead, cranial-caudal (CC) and medio-lateral oblique (MLO) views are obtained with DBT. Because breast compression is necessary in DBT in order to minimize tissue superposition, reduce X-ray scatter signal, and increase the amount of breast tissue in the field of view, processing of DBT projections in order to reconstruct a 3-D breast volume is not straightforward due to the lack

of orthogonal multiplanar views.^{36,37,38} Development of tridimensional reconstruction algorithms of DBT projections is beyond the scope of this work, and therefore, realistic breast modeling was alternatively carried out in a 2-step process in order to deal with the breast-deformation issue of DBT due to tissue compression.

First, the presence of tumors and the main tissues (tumoral tissue, fibroglandular tissue, and fatty tissue) in the region of interest were determined and marked out by physicians in both CC and MLO views in which dimensions, breast density, and the center of the tumor were determined. Tumor segmentation and 3-D reconstruction were carried out in 3-D Slicer in the original DBT images. Second, numerical breast phantoms available in a repository³⁹ and derived from T1-weighted magnetic resonance images of patients with no malignancy or other abnormalities were used to provide a decompressed model for the rest of the tissues of interest (fibroglandular and fatty tissue). Each phantom consists of a 3-D grid of cubic voxels of $0.5 \times 0.5 \times 0.5$ mm. The database of numerical phantoms was classified based on the standard tissue composition descriptors used by radiologists to classify X-ray mammograms according to the radiographic density of the breast. Four categories were defined according to the breast imaging reporting and data system (BI-RADS): (1) almost entirely fat (<25% glandular tissue), (2) scattered fibroglandular (25%-50% glandular), (3) heterogeneously dense (51%-75% glandular), and (4) very dense (>75% glandular).^{40,41}

In this work, a computational phantom was radiologically assigned to each patient based on the correlation of patient breast density grading with the categories of the BI-RADS. Breast tissue consists mainly of glandular parenchyma, connective tissue, and fatty tissue. Breast tissue and glandular parenchyma are radiologically considered as dense tissue. Patient 1 DBT images showed whitish appearance that pointed to a major glandular parenchyma proportion; hence, a very dense phantom was selected for this patient. A scattered fibroglandular phantom was used for patient 2, since dense tissue in DBT images showed a scattered pattern, which corresponded to a minor amount of glandular parenchyma. On the other hand, nondense mammographic areas (dark regions) were observed for patient 3, and therefore, a mostly fatty phantom was selected to represent this case. Three main tissues were considered for the phantoms, that is, skin, fibroconnective/glandular tissue, and fatty tissue for segmentation. Finally, in order to build a model of a realistic-anatomical breast with malignancies, the scale of the tumor segmentation corresponding to each patient was adjusted to fit the dimensions of the selected phantom; then, the reconstructed tumor was embedded into the selected computational breast phantom, keeping its original position inside the breast. This position was determined in its corresponding DBT image. This methodology allowed the development of a 3-D anatomical model of a patient-specific decompressed breast as shown in Figure 1. Table 1 shows the patients' and tumors' anatomical properties considered in order to build the breast models.

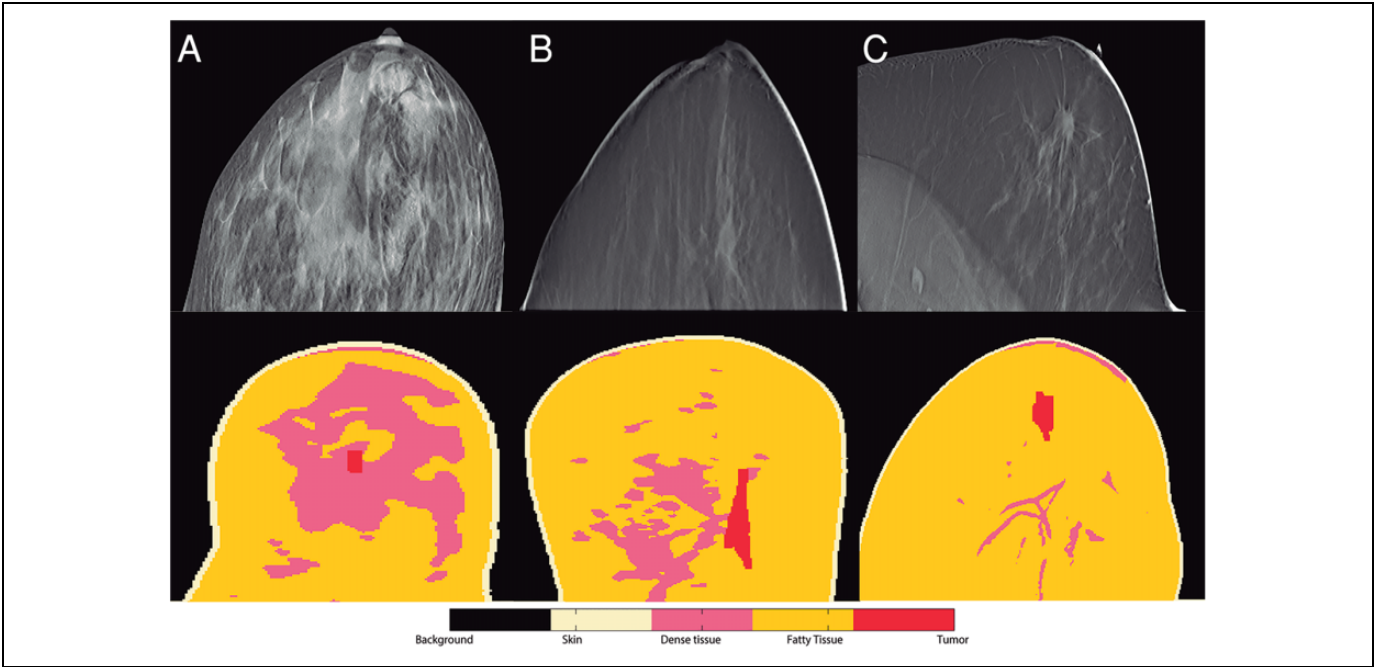


Figure 1. Breast Models. A, Craniocaudal (CC) view of a digital breast tomosynthesis of patient 1 and corresponding axial view of a very dense phantom analogue to CC view. B, Craniocaudal view of patient 2 and corresponding axial view of a scattered fibroglandular phantom. C, Medio-lateral-oblique view of patient 3 and corresponding sagittal view of a mostly fatty phantom analogue to medio-lateral oblique (MLO) view.

Table 1. Properties of the Anatomical Breast Models.

P ^a	Age	Location	Tumors			Phantom		
			#	Size, mm	Volume, cm ³	Type	Density	Volume Size, pixels
1	67	Left breast	1	4.4 × 9.1 × 11.5	0.46	III	Very dense	215 × 328 × 212
2	55	Left breast	1	38 × 9.6 × 8.5	3.10	II	Scattered fibroglandular	258 × 253 × 251
3	54	Left breast	1	29 × 9.5 × 18.5	5.10	I	Almost entirely fat	310 × 355 × 253

^aPatient.

Patient-Specific Treatment Planning

An efficient treatment of deep-seated invasive tumors with surgical resection requires the eradication of 10 mm of tissue surrounding the target tumor in order to reduce the probability of recurrences.⁴² This surrounding tissue is considered as a safety margin, and it must be taken into account along with the breast target tumor in each patient to develop the patient-specific treatment planning with electrochemotherapy.

Clinical cases differ from patient to patient in tumor size, tumor location, breast density, and dielectric properties of the tissues of interest; therefore, it was our purpose to determine first whether deep-seated invasive ductal carcinomas along with tissue into a safety margin of 10 mm may be eligible for their treatment with electrochemotherapy through the use of an universal electrode array, and second, the most effective electrode configuration and the electric protocol to be applied in that particular case. For this purpose, 3 sets of electrodes corresponding to 12 electrode arrays were proposed in this work. Electrode arrays in the different sets own the same number of

needles (4, 5, and 6) and the arrangement of needles (delta, diamond, and star), but they differ in distance among the electrodes as described in Figure 2 and Table 2. Number of needles ranges from 4 to 6 in order to investigate whether a sufficient electric field can be generated through the minimal number of electrodes and hence requiring fewer needle punctures. Variation in distance among the electrodes was proposed to fulfill a complete coverage of the tumors in the 3 patients according to their particular dimensions and geometries. However, it is our purpose to establish a suitable electrode array with a fixed-geometry configuration, which may cover target tissues in any clinical scenario of patients with IDC, based on the analysis of the 12 electrode arrays in the 3 patients reported in this work. In the clinical practice, handle of electrodes must remain the same for all electrode arrays, and selection of a particular electrode array shall depend on the dimensions of the target tumor. Needles' diameter in all arrays was 1.2 mm, and their active length varied depending on the tumor size as shown in Table 2, where C-P refers to the distance from the intratumoral–central electrode to the peripheral electrodes, P-P refers to the distance

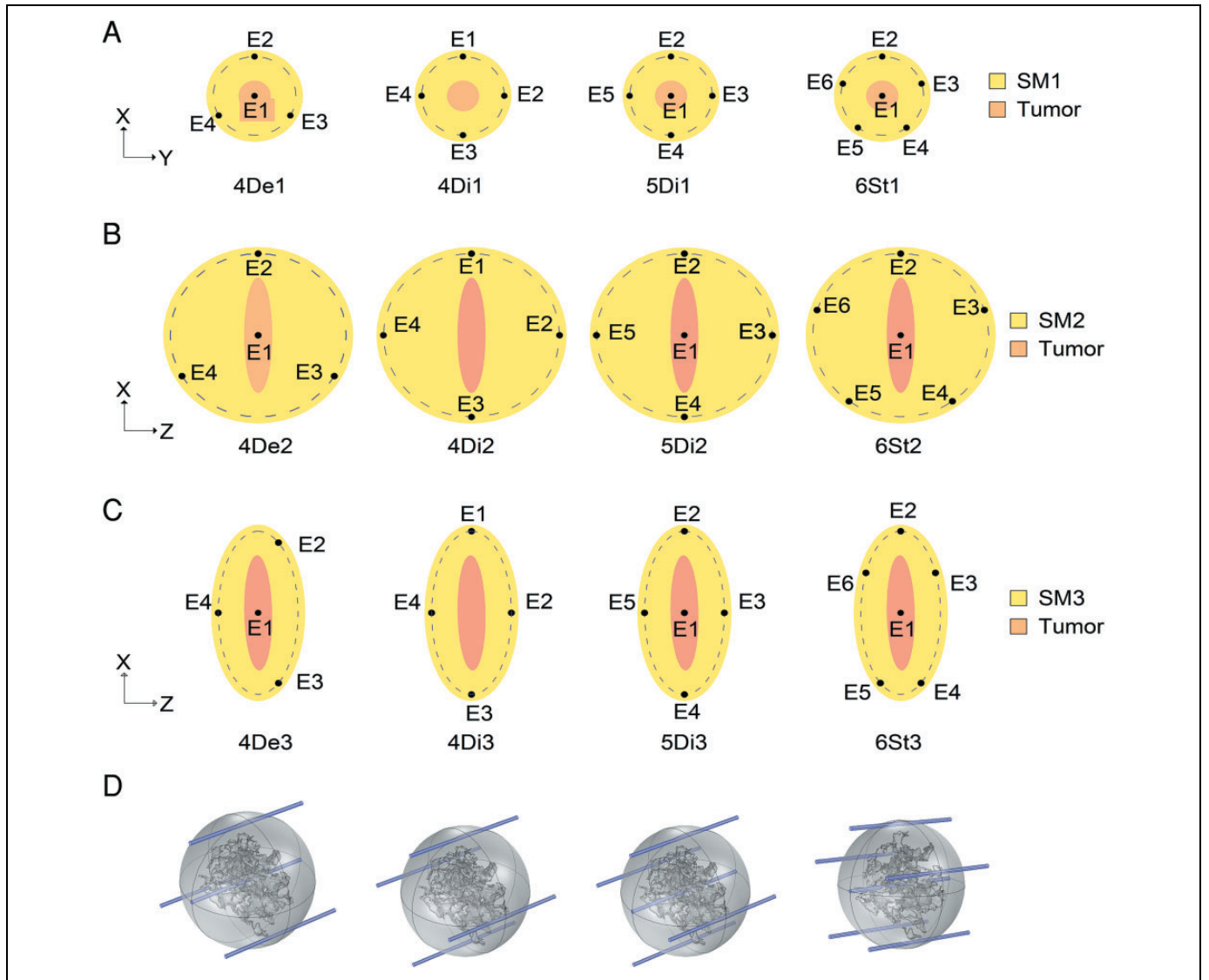


Figure 2. Topside view of (A) electrode set 1 for the treatment of a breast tumor (red) in patient 1 and a spherical safety margin tissue (SM1). (B) Electrode set 2 for the treatment of a breast tumor (red) in patient 2 and a spherical safety margin tissue (SM2). (C) Electrode set 3 for the treatment of a breast tumor (red) in patient 2 and an elliptic safety margin tissue (SM3). (D) Three-dimensional visualizations of the tumor embedded into a safety margin and the 4 electrode configurations; delta configuration, 4-needle diamond configuration, 5-needle diamond configuration, and 6-needle star configuration.

between peripheral electrodes only, and D refers to the distance between electrodes forming diagonals.

Electrode Arrays

In order to determine a suitable treatment protocol with electrochemotherapy for every clinical case and establish the coverage of the 3 target tissues, 4 needle-electrode configurations were used as an initial basis for each patient. Target tissues included the tumoral tissue in addition to the fatty and breast tissue comprised within a surrounding safety margin of 10 mm in diameter. Based on the number of needles (4, 5, or 6) and their configuration geometry (delta [De], diamond [Di], and star [St]), these original arrays were called 4De1, 4Di1, 5Di1,

and 6St1, Figure 2A. It is worth noting that for the diamond configuration, 2 electrode arrays were derived, that is, a 4-needle array without a central needle (4Di1) and a 5-needle array considering an intratumoral needle (5Di1). The safety margin for this set was considered as a sphere placed in the tumor center. Dimensional properties of these arrays are listed in Table 2. It can be seen that the distance between electrodes in the original array was appropriate to cover the tumoral volume of the first patient. However, tumors of the second and third patients were bigger, so in order to improve target coverage, the distance between the needles was increased resulting in 2 additional arrays. Electrode set 2 consists of an enlarged version of the electrode set 1 considering the safety margin as a sphere. Electrodes in this set were called 4De2, 4Di2, 5Di2, and 6St2 as

Table 2. Properties of the Needle-Electrode Arrays.

No. Needles	Configuration	Array	Symbol ^a	Active Length, mm	Distance ^b , mm		
					C-P	P-P	D
4	Delta	Original	4De1	15	13.0	22.5	–
		Enlarged	4De2	20	27.0	46.8	–
		Ellipse	4De3	20	24.1	29.7	–
	Diamond				12.2	46.5	
		Original	4Di1	15	–	18.4	26.0
		Enlarged	4Di2	20	–	38.2	54.0
		Ellipse	4Di3	20	–	29.6	54.0
							24.5
5	Diamond	Original	5Di1	15	13.0	18.4	–
		Enlarged	5Di2	20	27.0	38.2	–
		Ellipse	5Di3	20	27.0	29.6	–
					12.2		
6	Star	Original	6St1	15	13.0	15.3	–
		Enlarged	6St2	20	27.0	31.7	–
		Ellipse	6St3	20	27.0	17.4	–
					17.0	36.7	
					24.1	12.5	

^aSymbols indicate the number of needles (4, 5, 6), the array configuration (De = Delta, Di = Diamond, St = Star), and the electrode set marker (1 refers to the original electrode array, 2 refers to the enlarged electrode array, 3 refers to the ellipse electrode array).

^bC-P refers to the distance from the central-intratumoral electrode to the peripheral electrodes, P-P refers to the distance between peripheral electrodes, and D refers to the distance between opposite electrodes in diamond configuration.

shown in Figure 2B. Based on the dimensions of the tumor of patients 2 and 3, a safety margin with an ellipsoidal geometry was used in set 3, since it fit better the boundaries of the tumor. Electrode arrays in this set were called 4 needle-delta configuration-set 3 (4De3), 4 needle-diamond configuration-set 3 (4Di3), 5 needle-diamond configuration-set 3 (5Di3), and 6 needle-star configuration-set 3 (6St3) as shown in Figure 2C.

Electric Field Calculation

One of the objectives of this work was to determine whether it was feasible to treat deep-seated invasive ductal carcinomas effectively with electrochemotherapy through the use of a set of electrodes of fixed geometry. It has been reported that in order to achieve a successful ECT, reversible electroporation of tumor cells must be reached, so chemotherapeutic drugs are allowed to enter the cell and cause its death. Furthermore, IRE cannot be avoided, mostly in the periphery of the electrodes; therefore, contribution of IRE in cell death may be significant, but it may still be tolerated for ECT.³¹ Taking this into consideration, pairs of needles in the different electrode arrays were sequentially set to voltage until all combinations of unique pairs were activated, setting boundary conditions for voltage as an anode and a cathode during each simulation. For the electrode configurations with a central needle, the central needle was first set as an anode paired off with peripheral needles considered as cathodes in the safety margin; subsequently, only

Table 3. Dielectric Properties of Tissues in the Breast Models.

Tissue	Initial conductivity (σ_0) [S/m]	Final conductivity (σ_f) [S/m]	Threshold Electric Field [V/cm]	
			RE ^a	IRE ^b
Skin	0.170	0.170	400	800
Fibroconnective/glandular	0.085	0.340		
Fatty	0.025	0.100		
Tumor	0.425	1.700		

^aThreshold electric field for reversible electroporation in breast models.

^bThreshold electric field for irreversible electroporation in breast models.

peripheral electrodes were switched as anode and cathode, respectively. For configurations lacking a central needle (ie, 4Di1, 4Di2, and 4Di3), electrodes were commuted as anode and cathode in 6 possible combinations formed by adjacent and opposite needles. Initial voltage values were applied between each pair of electrodes in the different arrays. Depending on the tissue coverage resulting from this first simulation, voltage was varied until the target volumes were covered by an electric field magnitude above the reversible electroporation threshold in order to find the most appropriate treatment protocol for each patient.

Depending on the location of the tumor in the breast and the ease of needle insertion into the target tissue, the arrays were determined to be inserted normal to the axial plane for patients 1 and 2 and normal to the sagittal plane for patient 3. All models were computed in COMSOL Multiphysics (version 5.0, COMSOL, Sweden) with an algorithm written in Matlab (version R2013b; Mathworks, Natick, Massachusetts, USA) in order to establish the electric field distribution in the regions of interest. Visualization approach reported by Zupanic *et al* was used to extract the results and quantitatively compare the models based on the electroporation cross-section images, and the cumulative coverage of tissues by electric fields after the complete sequence of pulses has been applied. Cumulative coverage was displayed as an electric field histogram similar to dose-volume histograms used in radiation therapy planning. Electric field histograms were calculated for the 3 target tissues. All tissues were considered as isotropic with electrical conductivity values reported in the literature,^{31,43–45} and changes in conductivity due to electroporation were taken into account as shown in Table 3.

Results

Different electroporation protocols for each 1 of the 12 electrode arrays were used for the treatment of breast malignancies and surrounding tissue inside a safety margin of 1 cm around the tumor edge. The volumes of target tissues corresponding to the safety margin for each patient depended on the breast density and the phantom type used; total volumes of each tissue are listed in Table 4. Global electroporation results obtained for each patient are shown in Supplemental Table A. In

Table 4. Volumes of Target Tissues.

Patient	Volume of Target Tissues[cm ³]		
	Breast Tissue	Fatty Tissue	Tumor
1	10.20	3.76	0.46
2	5.16	19.73	3.10
3	1.05	26.58	5.10

Supplemental Table A, the first column shows the corresponding patient, and acronyms in the second column indicate the number of needles which we assumed as an indicator of invasiveness. Voltages between the different pairs of electrodes in the third column show the activation of electrode pairs. Percentage of tissue coverage in the fourth column indicates reversibly and irreversibly electroporated tissues, where breast and fat tissue correspond to the safety margin volume. Finally, the last column reports electric current obtained for each electroporation protocol. The most efficient treatment protocols obtained for each patient and each 1 of the 12 electrode arrays regarding the generation of an electric field magnitude above to the reversible electroporation threshold, and the coverage percentage of the 3 tissues of interest are shown highlighted in light red.

It has been reported that successful medical application of ECT requires the achievement of optimal parameters in the whole target tissue while keeping healthy tissue damage at a minimum.³¹ Nevertheless, in this work, healthy tissue constituting the safety margin was subjected to electroporation for the treatment of potential micro-metastases or tumor outgrowths not visible in imaging. The most efficient electrode array was selected for each patient hierarchically, taking into account the following criteria: (1) percentage of tumor volume reversibly electroporated; (2) percentage of tumor volume irreversibly electroporated; (3) percentage of treated safety margin volume; (4) minimal invasiveness, that is, minimal number of electrodes; (5) minimal activated electrode pairs; and (6) minimal electric current. Selection criteria are in accordance with the literature.³¹ The best electrode arrays are listed in Table 5, according to the hierarchic selection criteria applied to the global results reported in Supplemental Table A. The best electric protocols are reported as the voltage applied between central electrodes and peripheral electrodes (C-P), peripheral electrodes (P-P), and opposite electrodes (D, in 4-needle diamond configuration). The percentage of the target tissue covered between reversible and IRE thresholds and the average electric current between all pairs of activated electrodes are reported. It can be seen that for a small tumor in patient 1, a 4-needle electrode array in diamond configuration (4Di1) was suitable to reversibly cover the complete tumor and more than 90% of the safety margin. Good results were obtained with a 4-needle electrode array in delta configuration (4De2) and 6-needle electrode array in star configuration (6St2), as they covered 100% of the tumor and more than 85% of the safety margin. For patient 2, 5-needle electrode array in diamond

configuration (5Di2), 6St2 and 4De2 showed comparable results regarding reversibly electroporated tissue coverage. 5Di2 electrode array generated the minor IRE. Similarly, for patient 3, 6St2, 5Di2, and 4De2 resulted to be the most efficient electrode arrays in a comparable manner, but 5Di2 electrode array required fewer pairs of active electrodes.

The most effective electroporation protocols from Table 5 were 1000 V and 2000 V pulses between peripheral and opposite needles, respectively, in 4Di1 electrode array for patient 1, 2000 V pulses between C-P needles in 5Di2 electrode for patient 2, and 3000 V pulses between C-P needles in 6St2 electrode for patient 3. These protocols were used to determine the electric field histograms for the 3 target tissues (tumor, fatty, and breast tissue in the safety margin) as shown in Figures 3 to 5. Electric field histograms show the volume fraction of tissue (1 = 100%) covered at a certain electric field strength. A complete coverage was expected to be reached above 400 V/cm, whereas the tissue volume covered above 800 V/cm had to be kept at the minimum to minimize IRE. Tumor coverage in Figure 3 shows that an efficient electroporation (100% coverage above 400 V/cm) of a small tumor in patient 1 may be achieved with electrode 4Di1. Tumors from patients 2 and 3 were bigger than that from patient 1 and hence more difficult to reversibly electroporate, covering 98.9% and 98.6% of these tumors with 5Di2 and 6St2, respectively, with an electric field above 400 V/cm. It is worth noting that coverage of the tissues in the safety margin changed for the different breast densities due to the different dielectric properties of the tissues. Fatty tissue was easier to cover completely by fields above the reversible electroporation threshold (shown in Figure 4) than breast tissue (shown in Figure 5). At the same time, fatty tissue was also more susceptible to IRE than breast tissue.

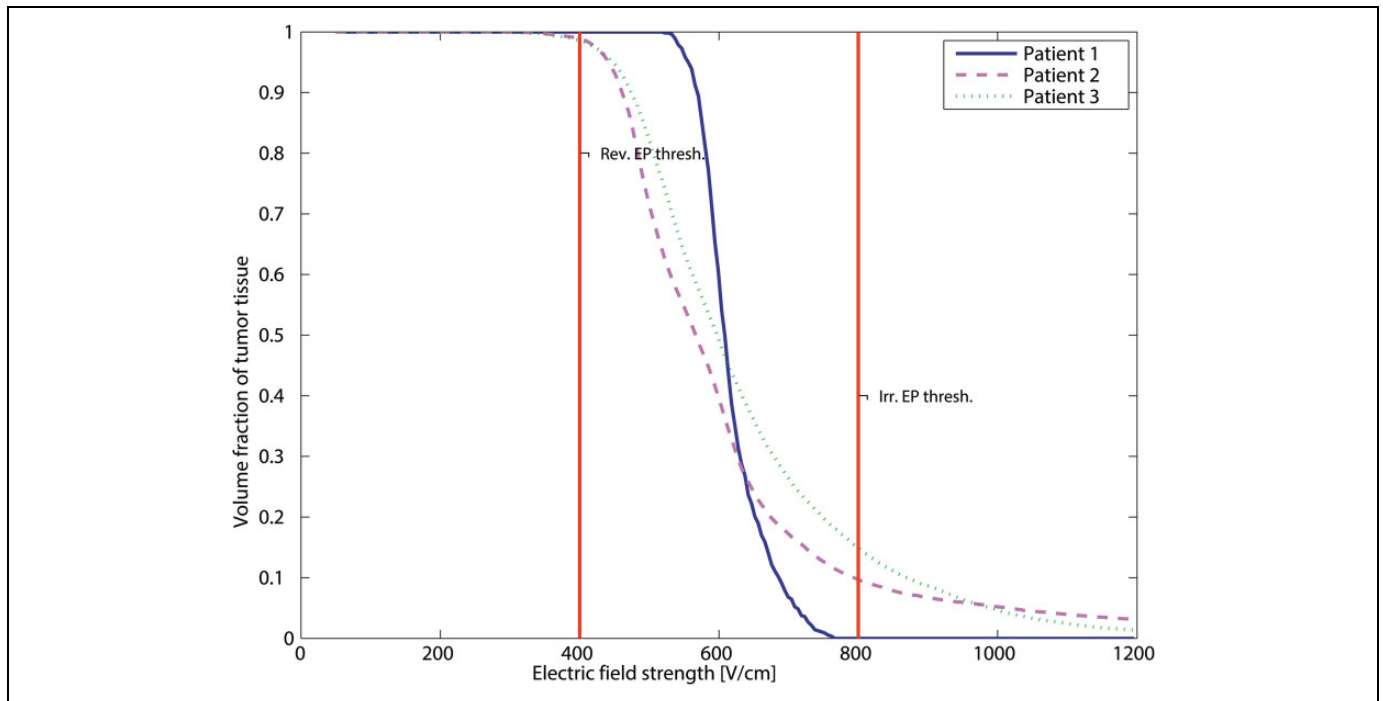
Electroporation color maps obtained for the most efficient protocol applied to each of the 3 breast models are shown in Figure 6. Irreversibly electroporated areas are marked in magenta, color blue represents reversibly electroporated areas in the tumors, and green shows reversibly electroporated areas in the safety margin tissues. Nontreated areas, that is, points where reversible electroporation threshold was not reached, appear uncolored.

Discussion

Twelve electrode arrays corresponding to 4 different configurations were used to evaluate the feasibility of treatment of invasive ductal breast carcinomas with electrochemotherapy. The results listed in Supplemental Table A show that the appropriate electrode array differs from patient to patient depending on the anatomical properties of the tissues of interest, that is, tumor size, breast density, and dielectric properties. This table also shows that a different efficient electric protocol was obtained for every patient. On the one hand, the treatment of a small tumor, in the case of patient 1, through an electrode with 4 needles in a diamond array (4Di1, set 1) and the activation of the peripheral needles only, was enough to cover the

Table 5. Effective Electroporation Protocols for the Treatment of Target Tissues.

		Voltage ^b [V]			Tissue Coverage [%]						
P ^a	Electrode Array	C-P	P-P	D	Tumor		Breast		Fat		e ^c [A]
					RE ^c	IRE ^d	RE	IRE	RE	IRE	
1	4Di1	–	1000	2000	100	0	95.1	22.9	99.8	48.4	3.5
	4De2	2000	1500	–	100	30.2	85.3	11.0	90.6	10.1	3.2
	6St2	1500	3000	–	100	33.5	85.0	6.2	91.8	6.6	4.3
2	5Di2	2000	–	–	98.9	9.7	96.7	16.9	99.2	28.1	7.9
	6St2	2500	2000	–	99.9	29.9	100	51.0	100	64.0	5.8
	4De2	3000	3000	–	99.8	60.3	99.6	48.8	99.8	62.3	7.5
3	6St2	3000	–	–	98.6	14.9	94.0	29.0	100	80.5	8.2
	5Di2	3000	–	–	97.8	15.4	92.1	27.5	100	74.9	8.2
	4De2	3000	3000	–	95.7	14.2	88.2	22.7	100	59.4	6.1

^aPatient.^bVoltage applied between central electrodes and peripheral electrodes (C-P), peripheral electrodes (P-P), and opposite electrodes (D) in 4-needle diamond configuration.^cPercentage of tissue covered at the reversible electroporation threshold (RE = 400 V/cm).^dPercentage of tissue covered at the irreversible electroporation threshold (RE = 800 V/cm).^eAverage electric current between activated pairs of needles.**Figure 3.** Most efficient coverage of tumors in the 3 patients. Electrode 4Di1 covered 100% of tumor in patient 1 with 1000 V and 2000 V between peripheral and opposite needles. Electrode 5Di2 covered 98.9% of tumor in patient 2 with 2000 V between C-P needles. Electrode 6St2 covered 98.6% of tumor in patient 3 with 3000 V between C-P needles.

whole tissues of interest. In addition, delta and star configuration (4De2 and 6St) in electrode set 2 resulted in effective target coverage. It is worth noting that as the tumors become bigger, as for the cases for patients 2 and 3, this electrode array (4Di1, set 1) was the least efficient configuration, since none of the tissues of interest got completely covered. On the other hand, efficient protocols for patient 2 were obtained with arrays in set 2 (6St2 and 4De2) and set 3 (4De3 and 6St3). It was

observed that the use of an electrode array following a tumor-specific safety margin geometry which was in turn selected based on the tumor dimensions (ideally elliptic for tumor in patient 2) resulted in optimal outcomes. Effective coverage for patient 3 was obtained with electrode arrays in set 2 (6St2, 5Di2, 4De2). Contrary to the results obtained for patient 1 with the array 4Di1, 4-needle diamond configuration in any of the sets, that is, 4Di1, 4Di2, and 4Di3, resulted in the least effective

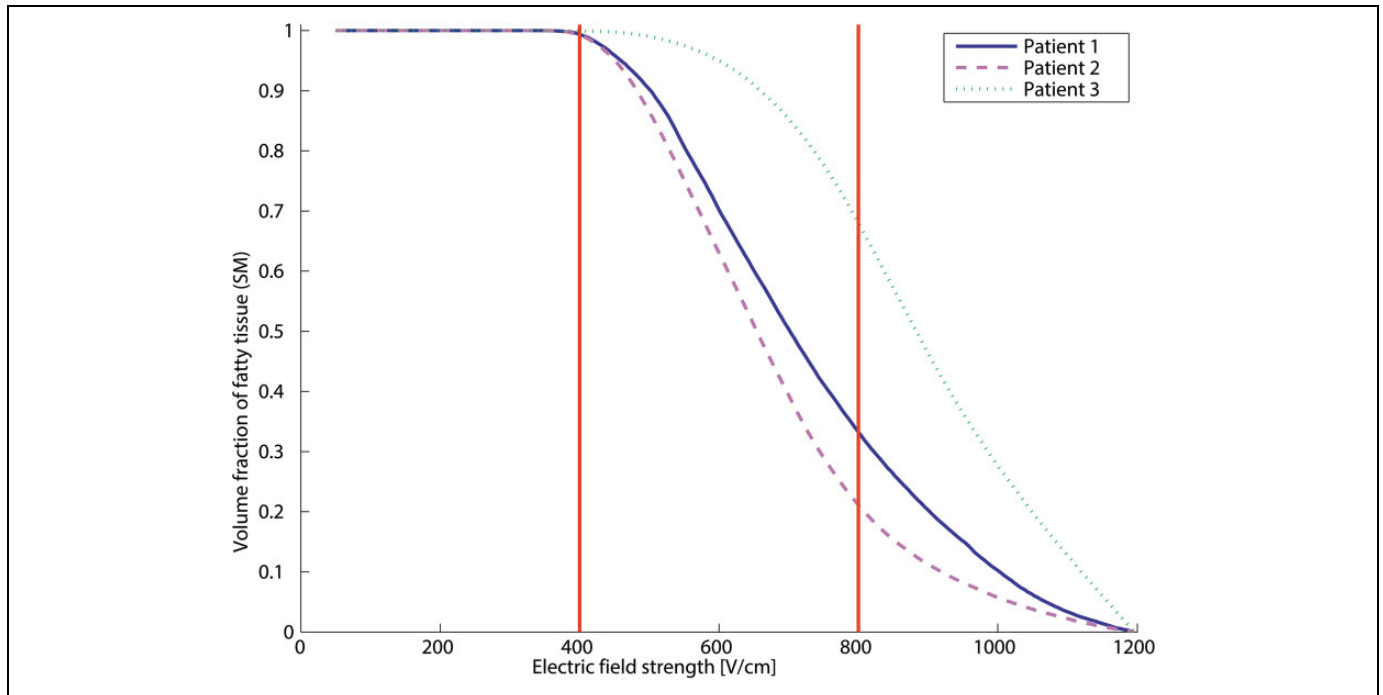


Figure 4. Most efficient coverage of fatty tissue in the safety margin for the 3 patients. Electrode 4Di1 covered 99.8% of fatty tissue in patient 1 with 1000 V and 2000 V between peripheral and opposite needles. Electrode 5Di2 covered 99.2% of fatty tissue in patient 2 with 2000 V between C-P needles. Electrode 6St2 covered 100% of fatty tissue in patient 3 with 3000 V between C-P needles.

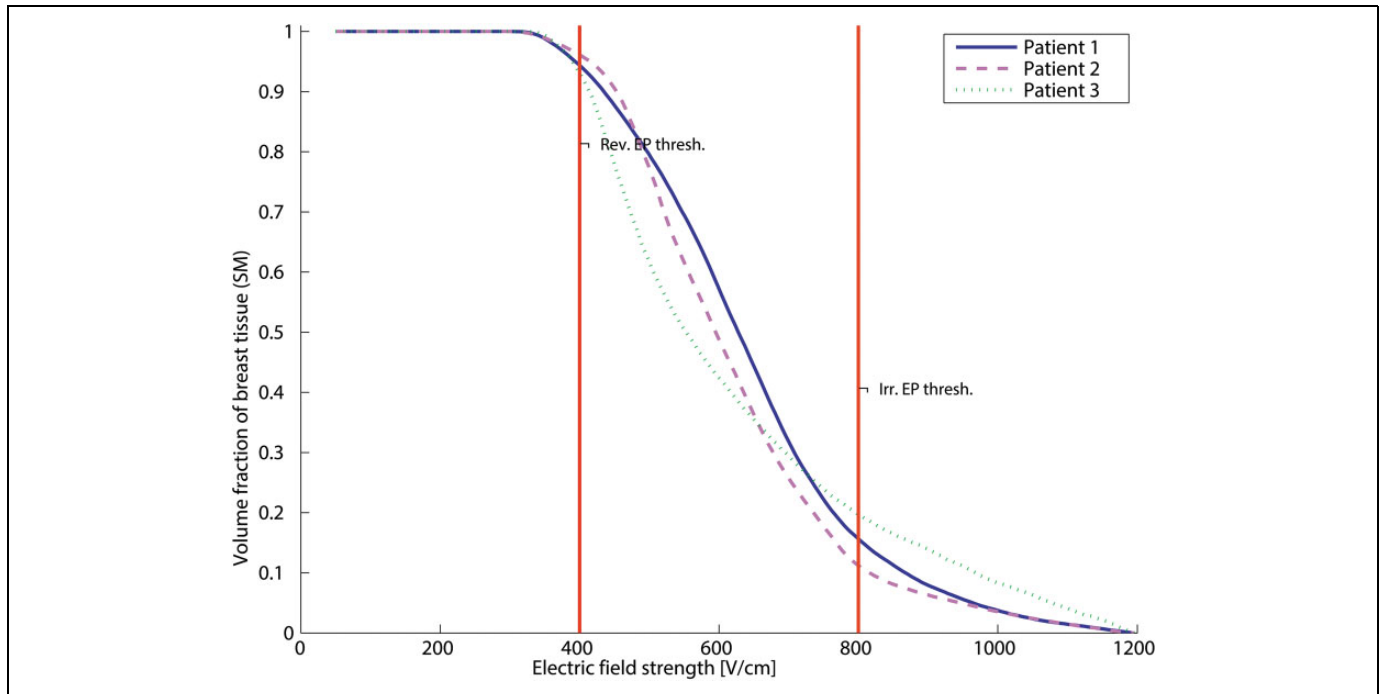


Figure 5. Most efficient coverage of breast tissue in the safety margin for the 3 patients. Electrode 4Di1 covered 95.1% of breast tissue in patient 1 with 1000 V and 2000 V between peripheral and opposite needles. Electrode 5Di2 covered 96.7% of breast tissue in patient 2 with 2000 V between C-P needles. Electrode 6St2 covered 94% of breast tissue in patient 3 with 3000 V between C-P needles.

arrays for the treatment of the target lesions even if the voltage was increased to the maximum value (3000 V) provided by current electroporation systems. Noticeably, an enlarged

version of the original electrode set used in patient 1, was the most appropriate set of electrodes for both patients 2 and 3 and a good alternative for patient 1 also. It is worthy to mention that

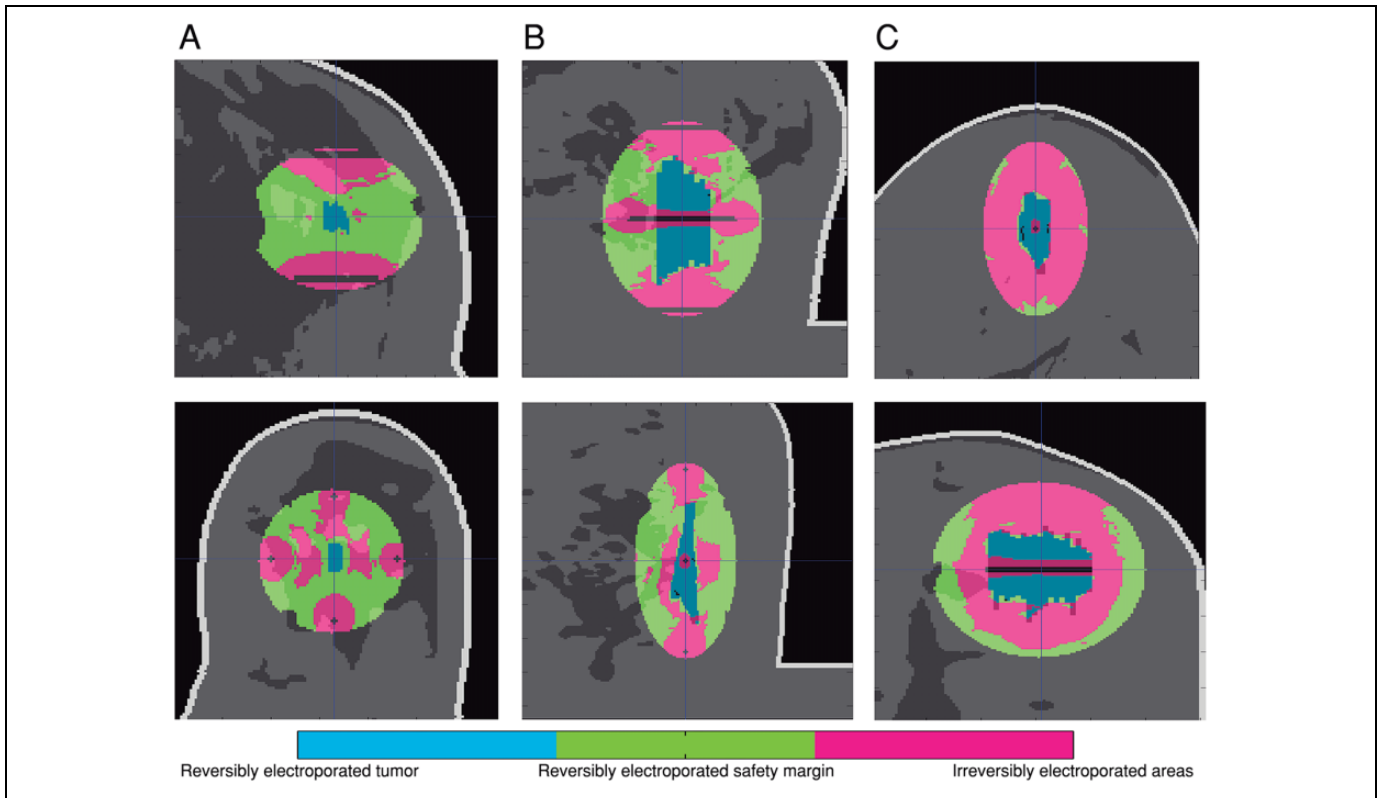


Figure 6. Visualization of electroporation reached in the target tissues of (A) patient 1, (B) patient 2, and (C) patient 3. Magenta color represents irreversibly electroporated regions, green shows reversibly electroporated regions in the safety margin (fatty tissue and breast) and blue indicates reversibly electroporated areas in the tumors. Nontreated areas in the models are uncolored.

for big tumors such as those in patients 2 and 3, a complete coverage of target tissues was harder to obtain if compared to the coverage of small tumors, but efficient coverage is possible to achieve.

Tissue dielectric property ratios used in this work were considerable ($\sigma_{\text{tumor}}/\sigma_{\text{breast tissue}} = 5\sigma_{\text{tumor}}/\sigma_{\text{fatty tissue}} = 17$), making electroporation a challenging process and hence requiring high-voltage values to achieve an efficient treatment. Based on the results reported in this work, it would be possible to use a fixed set of electrodes (4De2, 5Di2, and 6St2) to effectively treat invasive breast ductal carcinomas in the range of 1 to 5 cm³ with electrochemotherapy. Regarding the electrode-manufacturing issue, our results indicate that producing 2 electrode arrays (4De2 and 6St2) would be enough to treat invasive breast ductal carcinoma. This reduces meaningfully the complexity of manufacturing and device certification processes.

Further efforts aimed at imaging reconstruction of DBT views are required so that more accurate breast models can be obtained, since the breast models presented in this work consisted of interpolations of data in the DBT images in order to deal with the tissue compression issue. In addition, research with variations in the electrode positioning is encouraged in order to compare the results with the outcomes presented here. A comparison between the most effective electrode arrays (4De2, 5Di2, and 6St2) and the commercial hexagonal

electrode array with a central needle, manufactured by IGEA S.p.a (Carpi, Italy),⁸ would be useful in order to determine whether the number of needles may be reduced without jeopardizing the effectiveness of the treatment.

There are 2 articles addressing the treatment of primary breast cancer with ECT. Tumors in both cases can be reached by commercial electroporators and electrodes.^{29,30} Future acceptance of electrochemotherapy into medical practice as a first-line treatment of primary deep-seated breast tumors and possible replacement of conventional neoadjuvant chemotherapy and surgical procedures shall take into account advantages, drawbacks, and limitations of this procedure. Advantages include the reduction in antineoplastic drug dosage, local therapy administration instead of a systemic route, and hence the reduction in adverse effect of conventional chemotherapy (myelosuppression), potential displacement of neoadjuvant chemotherapy and/or radical mastectomy, treatment enhancement of triple negative lesions for which hormone therapy, and use of drugs that target estrogen, progesterone, and HER-2 receptors are ineffective, an apoptotic process would be induced in the major part of the target tissues contributing to a beneficial immune response.

Drawbacks

Drug resistance contribution through activation of multiple drug resistance pumps due to low-drug concentration if

multiple ECT sessions are required and inflammatory response associated with necrosis achieved in irreversibly electroporated regions.

Limitations

Determination of patient-specific breast dielectric properties in order to accurately model electroporation of target tissues, accomplishment of image-guided electrode positioning according to the treatment planning, and development of suitable hardware and electrodes that provide enough energy to deliver the electric protocol determined by the treatment planning.

Conclusion

The development of realistic breast models combining the use of computational breast phantoms and patient-specific tumor reconstruction is presented in this work as a novel approach to the modeling of electroporation of invasive breast ductal carcinomas diagnosed by DBT imaging. In order to achieve a sufficient electric field distribution in the tumor and a surrounding safety margin composed of fibroglandular breast tissue and fatty tissue, 3 sets of electrodes consisting of 12 electrode arrays were investigated.

The outcomes showed that an efficient average coverage percentage of the tissues of interest (tumor and safety margin) in the 3 patients was achieved with 3 main electrode arrays: 4 needles in a delta configuration 4De2 (tumor: 98.50%, breast tissue: 91.03%, fatty tissue: 96.80%), 5 needles in a diamond configuration 5Di2 (tumor: 98.76%, breast tissue: 86.53%, fatty tissue: 95.50%), and 6 needles in a star configuration 6St2 (tumor: 99.50%, breast tissue: 92.96%, fatty tissue: 97.20%). Consequently, we can conclude that a single-electrode array seems unlikely to treat effectively all breast ductal carcinomas with electrochemotherapy, but a group of 3 electrode arrays may be sufficient to cover the target tissues when treating this disease. Although a complete coverage of target tissues in large tumors, as it was the case for patients 2 and 3, was difficult to achieve, it should be considered that these tumor dimensions are representative of most of the current stages detected in Mexican patients with breast cancer. These outcomes could probably be extrapolated to any population with an effective response to the treatment; however, its effectiveness may be potentiated if the disease is detected at an early stage. Finally, outcomes obtained in this work encourage the use of electrochemotherapy, which has fewer unwanted side effects than the systemic chemotherapy, such as high toxicity and myelosuppression, for the treatment of invasive breast ductal carcinoma. We imply that it is possible that in future this method may displace neoadjuvant chemotherapy and/or surgery in the treatment of breast cancer and probably be considered as a first-line treatment of primary tumors. Nevertheless, enrollment of patients and experimental application of the method presented in this work conducting a clinical trial will be required to validate this hypothesis.

Acknowledgments

The research was conducted in the scope of LEA EBAM (French-Slovenian European Associated Laboratory: Pulsed Electric Fields Applications in Biology and Medicine). Study was performed within Infrastructure Programme: Network of research infrastructure centers at University of Ljubljana (MRIC UL IP-0510).



Declaration of Conflicting Interests

The author(s) declared the following potential conflicts of interest with respect to the research, authorship, and/or publication of this article: Damijan Miklavčič holds patents on electrochemotherapy that have been licensed to IGEA S.p.a (Carpi, Italy) and is also consultant to various companies with interest in electroporation based technologies and treatments. The other authors have no competing interests.

Funding

The author(s) disclosed receipt of the following financial support for the research, authorship, and/or publication of this article: A.L. Vera Tizatl thanks the National Council for Science and Technology (CONACYT, Mexico) for the scholarship granted. Authors thank the National Council for Science and Technology (CONACYT, Mexico) for the support received with project CONACYT-F-Salud 2013-I-201590, 201256, project CSIC-COOPB20166 and Project EMHE-CSIC 200022. The authors acknowledge the financial support from the Slovenian Research Agency (ARRS (research core funding No. P2-0249, and project "Development and validation of treatment planning methods for treating cancer with electroporation based therapies" Z3-7126).

ORCID iD

Damijan Miklavčič, PhD  <http://orcid.org/0000-0003-3506-9449>
Bor Kos, PhD  <http://orcid.org/0000-0001-6219-7046>

Supplemental Material

Supplemental material for this article is available online.

References

1. Masson Doyma, México SA, ed. *Consenso Mexicano sobre diagnóstico y tratamiento del cáncer mamario*. Mexico City, Mexico: Elsevier; 2015.
2. Types of breastcancer. <http://www.breastcancer.org/symptoms/types>. Updated November 9, 2016, Accessed December 14, 2016.
3. Stewart BW, Wild C, eds. *World Cancer Report 2014*. Lyon, France: International Agency for Research on Cancer; 2014.
4. Rems L, Miklavčič D. Tutorial. Electroporation of cells in complex materials and tissue. *J Appl Phys*. 2016;119(20):201101.
5. Davalos RV, Mir IL, Rubinsky B. Tissue ablation with irreversible electroporation. *Ann Biomed Eng*. 2005;33(2):223-231. doi:10.1007/s10439-005-8981-8.
6. Sersa G, Miklavcic D, Cemazar M, Rudolf Z, Pucihar G, Snoj M. Electrochemotherapy in treatment of tumours. *Eur J Surg Oncol*. 2008;34(2):232-240. doi:10.1016/j.ejso.2007.05.016.
7. Orlowski S, Belehradek J, Jr, Paoletti C, Mir LM. Transient electroporability of cells in culture. Increase of the cytotoxicity of anticancer drugs. *Biochem Pharmacol*. 1988;37(24):4727-4733. doi:10.1016/0006-2952(88)90344-9.

8. Miklavčič D, Mali B, Kos B, Heller R, Serša G. Electrochemotherapy: from the drawing board into medical practice. *Biomed Eng Online*. 2014;13(1):29. doi:10.1186/1475-925x-13-29.
9. Sersa G, Cemazar M, Miklavcic D. Antitumor effectiveness of electrochemotherapy with cis-Diamminedichloroplatinum(II) in mice. *Cancer Res*. 1995;55(15):3450-3455.
10. Yarmush ML, Golberg A, Serša G, Kotnik T, Miklavčič D. Electroporation-based technologies for medicine: principles, applications, and challenges. *Annu Rev Biomed Eng*. 2014;16(1):295-320. doi:10.1146/annurev-bioeng-071813-104622.
11. Kamensek U, Cemazar M, Lamprecht Tratar U, Ursic K, Sersa G. Antitumor in situ vaccination effect of TNF α and IL-12 plasmid DNA electrotransfer in a murine melanoma model. *Cancer Immunol Immunother*. 2018;67(5):785-795. doi:10.1007/s00262-018-2133-0.
12. Mir LM, Orlowski S, Belehradek J, Jr, Paoletti C. Electrochemotherapy potentiation of antitumour effect of bleomycin by local electric pulses. *Eur J Cancer*. 1991;27(1):68-72. doi:10.1016/0277-5379(91)90064-k.
13. Sersa G, Miklavcic D, Cemazar M, et al. Electrochemotherapy in treatment of tumours. *Eur J Surg Oncol*. 2008;34(2):232-240. doi:10.1016/j.ejso.2007.05.016.
14. Marty M, Sersa G, Garbay JR, et al. Electrochemotherapy—An easy, highly effective and safe treatment of cutaneous and subcutaneous metastases: results of ESOPE (European Standard Operating Procedures of Electrochemotherapy) study. *EJC Suppl*. 2006;4(11):3-13. doi:10.1016/j.ejcsup.2006.08.002.
15. Mali B, Jarm T, Snoj M, Sersa G, Miklavcic D. Antitumor effectiveness of electrochemotherapy: a systematic review and meta-analysis. *Eur J Surg Oncol*. 2013;39(1):4-16. doi:10.1016/j.ejso.2012.08.016.
16. Haberl S, Miklavcic D, Sersa G, Frey W, Rubinsky B. Cell membrane electroporation-Part 2: the applications. *IEEE Electrical Insulation Magazine*. 2013;29(1):29-37. doi:10.1109/mei.2013.6410537.
17. Campana LG, Galuppo S, Valpione S, et al. Bleomycin electrochemotherapy in elderly metastatic breast cancer patients: clinical outcome and management considerations. *J Cancer Res Clin Oncol*. 2014;140(9):1557-1565. doi:10.1007/s00432-014-1691-6.
18. Wichtowski M, Murawa D, Kulcenty K, Zaleska K. Electrochemotherapy in breast cancer—discussion of the method and literature review. *Breast Care*. 2017;12(6):409-414. doi:10.1159/000479954.
19. Matthiessen LW, Johannesen HH, Hendel HW, Moss T, Kamby C, Gehl J. Electrochemotherapy for large cutaneous recurrence of breast cancer: a phase II clinical trial. *Acta Oncol*. 2012;51(6):713-721. doi:10.3109/0284186x.2012.685524.
20. Miklavčič D, Serša G, Breclj E, et al. Electrochemotherapy: technological advancements for efficient electroporation-based treatment of internal tumors. *Med Biol Eng Comput*. 2012;50(1):1213-1225.
21. Edhemovic I, Breclj E, Gasljevic G, et al. Intraoperative electrochemotherapy of colorectal liver metastases. *J Surg Oncol*. 2014;110(3):320-327. doi:10.1002/jso.23625.
22. Cadossi R, Ronchetti M, Cadossi M. Locally enhanced chemotherapy by electroporation: clinical experiences and perspective of use of Electrochemotherapy. *Future Oncol*. 2014;10(5):877-890. doi:10.2217/fon.13.235.
23. Granata V, Fusco R, Piccirillo M, et al. Electrochemotherapy in locally advanced pancreatic cancer: preliminary results. *Int J Surg*. 2015;18:230-236. doi:10.1016/j.ijsu.2015.04.055.
24. Bianchi G, Campanacci L, Ronchetti M, Donati D. Electrochemotherapy in the treatment of bone metastases: a phase II trial. *World J Surg*. 2016;40(12):3088-3094. doi:10.1007/s00268-016-3627-6.
25. Wichtowski M, Potocki P, Kufel-Grabowska J, Streb J, Murawa D. Electrochemotherapy in the treatment of massive, multisite breast cancer metastasis to the skin and subcutaneous tissue: a case report. *Breast Care (Basel)*. 2016;11(5):353-355. doi:10.1159/000450869.
26. Kalavathy G, Sasi KS, Manohar PE, Sundararajan R. Electrochemotherapy makes resectable from unresectable and pain reduction in chest wall recurrence breast cancer of two patients. *J Cancer Prev Curr Res*. 2015;3(2):00074. doi:10.15406/jcpr.2015.03.00074.
27. Schmidt G, Juhasz-Böss I, Solomayer EF, Herr D. Electrochemotherapy in breast cancer: a review of references. *Geburtshilfe Frauenheilkd*. 2014;74(6):557-562. doi:10.1055/s-0034-1368538.
28. Sersa G, Cufer T, Paulin SM, Cemazar M, Snoj M. Electrochemotherapy of chest wall breast cancer recurrence. *Cancer Treat Rev*. 2012;38(5):379-386. doi:10.1016/j.ctrv.2011.07.006.
29. Cabula C. Neoadjuvant electrochemotherapy of breast cancer: our experience on first case treated in Italy. *Updates Surg*. 2012;65(4):325-328. doi:10.1007/s13304-012-0170-3.
30. Denzi A, Strigari L, Di Filippo F, et al. Modeling the positioning of single needle electrodes for the treatment of breast cancer in a clinical case. *Biomed Eng Online*. 2015;14(suppl 3):S1. doi:10.1186/1475-925x-14-s3-s1.
31. Neal RE, 2nd, Davalos RV. The feasibility of irreversible electroporation for the treatment of breast cancer and other heterogeneous systems. *Ann Biomed Eng*. 2009;37(12):2615-2625. doi:10.1007/s10439-009-9796-9.
32. Neal RE, 2nd, Singh R, Hatcher HC, Kock ND, Torti SV, Davalos RV. Treatment of breast cancer through the application of irreversible electroporation using a novel minimally invasive single needle electrode. *Breast Cancer Res Treat*. 2010;123(1):295-301. doi:10.1007/s10549-010-0803-5.
33. Zhang W, Wang W, Chai W, et al. Breast tissue ablation with irreversible electroporation in rabbits: a safety and feasibility study. *PLoS One*. 2017;12(7):e0181555. doi:10.1371/journal.pone.0181555.
34. Deipolyi AR, Golberg A, Yarmush ML, Arellano RS, Oklu R. Irreversible electroporation: the evolution of a laboratory technique to be used in interventional oncology. *Diagn Interv Radiol*. 2014;20(2):147-154. doi:10.5152/dir.2013.13304.
35. Zupanic A, Kos B, Miklavcic D. Treatment planning of electroporation-based medical interventions: electrochemotherapy, gene electrotransfer and irreversible electroporation. *Phys Med Biol*. 2012;57(17):5425-5440. doi:10.1088/0031-9155/57/17/5425.
36. Smith A. Fundamentals of breast tomosynthesis: improving the performance of mammography, 2012, 78967-12_WP-00007_

- FundmntlsTomo. <http://web.psmedical.it/DOC/Fundamentals.pdf>. Updated 2008, Accessed June 23, 2018.
37. Ertas M, Yildirim I, Kamasak M, Akan A. Digital breast tomosynthesis image reconstruction using 2D and 3D total variation minimization. *Biomed Eng Online*. 2013;12(1):112. doi:10.1186/1475-925x-12-112.
 38. Sechopoulos I. A review of breast tomosynthesis. Part II. Image reconstruction, processing and analysis, and advanced applications. *Med Phys*. 2013;40(1):014302. doi:10.1118/1.4770281.
 39. Zastrow E, Davis SK, Lazebnik M, Kelcz F, Van Veen BD, Hagness SC. Development of anatomically realistic numerical breast phantoms with accurate dielectric properties for modeling microwave interactions with the human breast. *IEEE Trans Biomed Eng*. 2008;5(12):2792-2800. doi:10.1109/tbme.2008.2002130.
 40. Numerical Breast Phantoms Repository. <http://uwcem.ece.wisc.edu/MRIdatabase/>. Accessed October 12, 2017.
 41. Sickles EA, D'Orsi CJ, Basset LW, et al. ACR BI-RADS® Mammography. In: ACR BI-RADS® Atlas. Breast Imaging Reporting and Data System. Reston, VA: American College of Radiology; 2013.
 42. Moran MS, Schnitt SJ, Giuliano AE, et al. Society of Surgical Oncology–American Society for Radiation Oncology Consensus Guideline on Margins for Breast-Conserving Surgery With Whole-Breast Irradiation in Stages I and II Invasive Breast Cancer. *Int J Radiat Oncol Biol Phys*. 2014;88(3):553-564. doi:10.1016/j.ijrobp.2013.11.012.
 43. Jossinet J. Variability of impedivity in normal and pathological breast tissue. *Med Biol Eng Comput*. 1996;34(5):346-350. doi:10.1007/bf02520002.
 44. Surowiec AJ, Stuchly SS, Barr JB, Swarup A. Dielectric properties of breast carcinoma and the surrounding tissues. *IEEE Trans Biomed Eng*. 1988;35(4):257-263. doi:10.1109/10.1374.
 45. Gabriel S, Lau RW, Gabriel C. The dielectric properties of biological tissues: III. Parametric models for the dielectric spectrum of tissues. *Phys Med Biol*. 1996;41(11):2271-2293. doi:10.1088/0031-9155/41/11/003.